Solution Synthesis of Thin Films in the SnO_2−In_2O_3 System: A Case Study of the Mixing of Sol−Gel and Metal-Organic Solution Processes

Mauro Epifani,*,† Raül Díaz,‡ Jordi Arbiol,‡ Pietro Siciliano,† and Joan R. Morante‡

CNR-IMM, Consiglio Nazionale delle Ricerche − Istituto per la Microelettronica ed i Microsistemi, Sezione di Lecce, via Arnesano, 73100 Lecce, Italy, and Departament d'Electrònica, Universitat de Barcelona, C. Martí i Franqués 1, 08028 Barcelona, Spain

Received October 10, 2005. Revised Manuscript Received December 7, 2005

Thin films with nominal molar compositions ranging from 98% In_2O_3−2% SnO_2 to 2% In_2O_3−98% SnO_2 were prepared by mixing solutions of Sn(II) 2-ethylhexanoate in butanol with In_2O_3 sols prepared by a chemical complexation-based sol−gel process. The starting solutions were characterized by Fourier transform infrared spectroscopy, while the thin films, prepared by spin coating on silicon substrates and subsequent heat treatments up to 500 or 800 °C, were characterized by X-ray diffraction, field emission scanning electron microscopy, Auger spectroscopy, Fourier transform infrared spectroscopy, high-resolution transmission electron microscopy, and electron energy loss spectroscopy. It was concluded that the main factor governing the film formation is the lack of cross-linking reactions between the Sn and In species in the starting solutions. This may result in phase separation already during the spinning stage, in particular, for compositions with comparable concentrations of the two components. During the heat treatment, In_2O_3 crystallization is favored and is able to prevent that of SnO_2 even when the concentration of the former is 10%. This result is explained by referring to the different chemistry involved in the solution processing of the Sn precursor with respect to the sol−gel processing of In_2O_3. Upon heat treatment up to 800 °C, a peculiar structure forms in the film with 30% In_2O_3, constituted by a mixture of nanocrystals of SnO_2, In_2O_3, and a mixed phase.

1. Introduction

Indium tin oxide (ITO) is an n-type semiconductor that presents high electrical conductivity and high optical transparency to visible light.[1] Thus, ITO thin films, prepared by various deposition techniques including chemical vapor deposition (CVD),[2] pulsed laser deposition,[3] magnetron sputtering,[4] and spray pyrolysis,[5] have been extensively used as hole-injecting anodes in organic light-emitting diodes (OLEDs)[6] and as electrode material in biosensing,[7] solar cell applications,[8] and gas sensing.[9] Recently, chemical processing of ITO thin films has been increasingly applied, taking advantage of the simple equipment required, the inexpensive precursors and their easy processing, and the possibility of simple deposition of thin films. The solution processing, including sol−gel, of several inorganic precursors such as $InCl_3$ and $SnCl_4$,[10] $SnCl_2$ and $In(OH)(CH_3COO)_2$,[11] $In(NO_3)_3 \cdot 5H_2O$ and Sn tetrachloride,[12] oxalate,[13] or acetate[14] has been proposed. The use of metal alkoxides is less frequently reported.[15] ITO powders have also been conveniently prepared from similar precursors, in particular by coprecipitation[16] and hydrothermal synthesis.[17] The choice of the

* Corresponding author. E-mail: mauro.epifani@le.imm.cnr.it.
† CNR-IMM.
‡ Universitat de Barcelona.

(1) (a) Li, C.; Zhang, D. H.; Han, S.; Liu, X. L.; Tang, T.; Zhou, C. *Adv. Mater.* **2003**, *15*, 143. (b) Soulantica, K.; Erades, L.; Sauvan, M.; Senocq, F.; Maisonnat, A.; Chaudret, B. *Adv. Funct. Mater.* **2003**, *13*, 553. (c) Gurlo, A.; Barsan, N.; Weimar, U.; Ivanovskaya, M.; Taurino, A.; Siciliano, P. *Chem. Mater.* **2003**, *15*, 4377. (d) Gonzalez, G. B.; Mason, T. O.; Quintana, J. P.; Warschkow, O.; Ellis, D. E.; Hwang, J.-H.; Hodges, J. P.; Jorgensen, J. D. *J. Appl. Phys.* **2004**, *96*, 3912. (e) Swint, A. L.; Bohn, P. W. *Langmuir* **2004**, *20*, 4076.
(2) Rykara, L. A.; Salum, V. S.; Serbinov, I. A. *Thin Solid Films* **1982**, *92*, 327.
(3) Zheng, J. P.; Kwok, H. S. *Appl. Phys. Lett.* **1993**, *63* (1), 1.
(4) Kwok, H. S.; Sun, X. W.; Kim, D. H. *Thin Solid Films* **1998**, *335*, 299.
(5) Korotcenkov, G.; Brinzari, V.; Schwank, J.; DiBattis, M.; Vasiliev, A. *Sens. Actuators, B* **2001**, *77*, 244.
(6) Kim, H.; Piqu, A.; Horwitz, J. S.; Mattoussi, H.; Murata, H.; Kafafi, Z. H.; Chrisey, D. B. *Appl. Phys. Lett.* **1999**, *74*, 3444.
(7) Brusatori, M. A.; Van Tassel, P. R. *Biosens. Bioelectron.* **2003**, *18*, 1269.
(8) Pla, J.; Tamasi, M.; Rizzoli, R.; Losurdo, M.; Centurioni, E.; Summonte, C.; Rubinelli, F. *Thin Solid Films* **2003**, *425*, 185.
(9) (a) Hu, J. Q.; Zhu, F. R.; Zhang, J.; Gong, H. *Sens. Actuators, B* **2003**, *93*, 175. (b) Patel, N. G.; Makhija, K. K.; Panchal, C. J.; Dave, D. B.; Vaishnav, V. S. *Sens. Actuators, B* **1995**, *23*, 49. (c) Jiao, Z.; Wu, M.; Gu, J.; Sun, X. *Sens. Actuators, B* **2003**, *94*, 216.
(10) (a) Stoica, T. F.; Stoica, T. A.; Vanca, V.; Lakatos, E.; Zaharescu, M. *Thin Solid Films* **1999**, *348*, 273. (b) Alam, M. J.; Cameron, D. C. *Surf. Coat. Technol.* **2001**, *142*−*144*, 776. (c) Ramanan, S. R. *Thin Solid Films* **2001**, *389*, 207.
(11) Seki, S.; Sawada, Y.; Nishide, T. *Thin Solid Films* **2001**, *388*, 22.
(12) Su, C.; Sheu, T.-K.; Chang, Y.-T.; Wan, M.-A.; Feng, M.-C.; Hung, W.-C. *Synth. Met.* **2005**, *153*, 9.
(13) Tomonaga, H.; Morimoto, T. *Thin Solid Films* **2001**, *392*, 243.
(14) Kim, S.-S.; Choi, S.-Y.; Park, C.-G.; Jin, H.-W. *Thin Solid Films* **1999**, *347*, 155.
(15) (a) Toki, M.; Aizawa, M. *J. Sol-Gel Sci. Technol.* **1997**, *8*, 717. (b) Stoica, T. F.; Teodorescu, V. S.; Blanchin, M. G.; Stoica, T. A.; Gartner, M.; Losurdo, M.; Zaharescu, M. *Mater. Sci. Eng. B* **2003**, *101*, 222.
(16) (a) Pramanik, N. C.; Das, S.; Biswas, P. K. *Mater. Lett.* **2002**, *56*, 671. (b) Kim, K. I.; Park, S. B. *Mater. Chem. Phys.* **2004**, *86*, 210.
(17) (a) Yanagisawa, K.; Udawatte, C.; Nasu, S. *J. Mater. Res.* **2000**, *15*, 1404. (b) Xu, H.-R.; Zhu, G.-S.; Zhou, H.-Y.; Yu, A.-B. *Mater. Lett.* **2005**, *59*, 19.

10.1021/cm0522477 CCC: $33.50
Published on Web 01/14/2006

precursors dictates the solution chemistry and, hence, the structure of the final material. In aqueous conditions, hydrolysis reactions are essential in determining the solution chemistry: while the presence of hydroxyl bonds may favor the mixing of the various species in the sol, on the other hand, the difference in the hydrolysis rates of the two metal ions will determine whether separated domains of each single element will form instead of heterobonds such as In−O−Sn.

When trying to deposit ITO films by mixing In_2O_3 and SnO_2 sols prepared from, respectively, $In(NO_3)_3$[18] and $SnCl_4$,[19] we observed that residual chlorine in the SnO_2 sol seriously affected the uniformity of thin films on oxidized silicon substrates. For overcoming this problem, a simple solution deposition was achieved, by using Sn(II) 2-ethylhexanoate dissolved in butanol. In this way, the sol−gel chemistry of the In precursor was mixed with the solution chemistry of the Sn precursor, so deviating remarkably from the previously described works. Since, to the best of our knowledge, the mixing of precursors with such properties has not been studied in detail, it seemed of extreme interest to consider the preparation of ITO films by this procedure as a case study of the mixing of precursors with different chemical properties. Moreover, while many studies can be found concerning the preparation of ITO materials with different compositions, there are only a few studies in the whole composition range, and they are limited to films prepared by other techniques such as spray pyrolysis[20] or RF plasma[21] on glass substrates.

In our work, both the starting solutions and the final ITO materials were systematically investigated in the whole range of nominal compositions, from 100% In_2O_3−0% SnO_2 to 0% In_2O_3−100% SnO_2. The precursor solutions and the films were characterized by Fourier transform infrared spectroscopy (FTIR), X-ray diffraction (XRD), field emission scanning electron microscopy (FE-SEM), Auger spectroscopy, high-resolution transmission electron microscopy (HRTEM), and electron energy loss spectroscopy (EELS). The results revealed the absence of interaction in the starting solution between the investigated indium and tin precursors. This is the key point in the subsequent film formation and evolution with the heat treatments, which generally proceed through phase separations already induced during the spin-coating stage. It will be shown that, due to the phase separations, peculiar film compositions may take place, composed of different oxide nanocrystals in the same film structure.

2. Experimental Section

For preparing thin films in the $SnO_2-In_2O_3$ system, precursor solutions of the two elements were mixed in such proportions to give a nominal composition, expressed as the molar percentage of the two oxides, ranging from 98% In_2O_3−2% SnO_2 to 2% In_2O_3−98% SnO_2. In the following, the composition will be indicated with the general label *x*I−*y*S, where *x* is the In_2O_3 percentage and *y* is the SnO_2 percentage. For compositions from 100I−0S to 50I−50S, the In_2O_3 precursor solution was prepared by a modified sol−gel process similar to that previously reported,[18] by dissolving 1 g of $In(NO_3)_3 \cdot 5H_2O$ in 15 mL of methanol, followed by the addition of acetylacetone (acacH) with an acacH:In molar ratio of 3. After 30 min since the addition of acacH, a concentrated (30 wt %) water solution of NH_3 was added in order to get a NH_3:In molar ratio of 2. Finally, 75 mg of cetyltrimethylammonium bromide (CTAB) was dissolved in the resulting sol for improving the adhesion of the film onto the silicon substrates. Then, the required amount of Sn(II) 2-ethylhexanoate was dissolved in 2.5 mL of butanol and this solution was mixed with the In_2O_3 sol. For compositions from 30I−70S to 0I−100S, the precursor solution of SnO_2 was prepared by dissolving 1.25 g of Sn(II) 2-ethylhexanoate in 7 mL of butanol, followed by the addition of 100 mg of CTAB. Then, the In_2O_3 sol was added in the required proportions, but in this case it was prepared without CTAB.

Thin films were deposited by spin coating onto oxidized (5600 Å SiO_2 layer) silicon substrates. Spin coating was carried out at 2000 rpm, followed by drying at 70 °C for 5 min and by heat treatment in a tubular oven in a flow of O_2, with a heating rate of 5 °C/min up to final temperatures ranging from 120 to 500 °C. After heat treatment at 500 °C, the film thickness, measured by a profilometer (Tencor Instruments, Alpha-Step IQ), was about 100 nm for 0I−100S (pure SnO_2) and 60 nm for 100I−0S (pure In_2O3), while it had intermediate values for the other compositions.

X-ray diffraction (XRD) patterns have been obtained with a Siemens D-500 X-ray diffractometer using Cu Kα radiation (λ = 1.5418 Å), with an operating voltage of 40 kV and a current of 30 mA. Data were collected in steps of 0.05° (2θ) from 10° to 80°. A grazing incidence angle of 2° was used for the acquisition.

The Fourier transform infrared (FTIR) spectroscopic measurements were carried out on the solutions with a Bomem MB-120 FTIR spectrometer, in a range from 350 to 4000 cm^{-1}, with a maximum resolution of 1 cm^{-1}. The samples were prepared by placing a drop of the solution on a KBr pellet and then evaporating the solvent at room temperature.

The Auger characterization has been done in a PHI SAM-670, scanning Auger nanoprobe system with Schottky field emission source and multichannel detector. The e-gun parameters were as follows: 10 keV to 10 nA with a residual pressure of 5×10^{-10} Torr.

An Hitachi S-4100 field emission scanning electron microscope with a theoretical resolution of 1.5 nm was used for the microscopic characterization of the samples. Typically, an acceleration voltage of 30 kV was applied and, for the samples with lower conductivity, a thin C film was evaporated to prevent artifacts.

High-resolution transmission electron microscopy (HRTEM) studies were carried out with a field emission gun microscope JEOL 2010F, which works at 200 kV and has a point-to-point resolution of 0.19 nm. Electron energy loss spectroscopy (EELS) spectra were obtained in a Gatan Image Filter (GIF 2000) coupled to the JEOL 2010F microscope. Spectra obtained achieved an energy resolution of 1.2 eV.

3. Results and Discussion

A. Preparation and Characterization of the Starting Solutions. The use of Sn 2-ethylhexanoate in the preparation of thin films is attractive for several reasons: the low cost and toxicity, the air stability, and the absence of chlorine residuals. Moreover, there are a limited number of reports about its use as a precursor to SnO_2 thin films.[22] As concerns

(18) Epifani, M.; Capone, S.; Rella, R.; Siciliano, P.; Vasanelli, L.; Faglia, G.; Nelli, P.; Sberveglieri, G. *J. Sol-Gel Sci. Technol.* **2003**, *26*, 741.
(19) Epifani, M.; Alvisi, M.; Mirenghi, L.; Leo, G.; Siciliano, P.; Vasanelli, L. *J. Am. Ceram. Soc.* **2001**, *84*, 48.
(20) Rozati, S. M.; Ganj, T. *Renew. Energy* **2004**, *29*, 1671.
(21) Lee, D. H.; Vuong, K. D.; Williams, J. A. A.; Fagan, J.; Condrate, R. A., Sr.; Wang, X. W. *J. Mater. Res.* **1996**, *11*, 895.

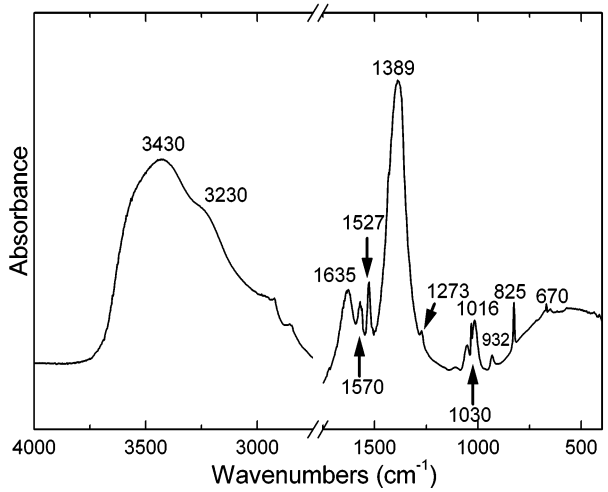

Figure 1. FTIR curve measured on a pure In_2O_3 sol.

Table 1. Peak Positions in Figure 1 and Related Assignments

peak position (cm^{-1})	assignment
3430	O−H stretching (broad band)
3230	NH_3 stretching in the In ammine complex ($+NH_4$ stretch)
1635	NH_3 degenerate deformation in the In ammine complex; H_2O band
1570	acetylacetonato band in the In complex
1527	acetylacetonato band in the In complex
1389	NH_3 symmetric deformation in the In ammine complex + nitrate mode
1273	acetylacetonato band in the In complex
1030	Methanol
1016	acetylacetonato band in the In complex
932	acetylacetonato band in the In complex
825	NO_3^- deformation
670	acetylacetonato band in the In complex + ν(In−O)

the preparation of the In_2O_3 sol, the use of acetylacetone was effective in limiting the condensation reactions after the base addition. In this way the deposition of uniform thin films was possible. This effect can be explained by referring to the formation of less condensed species in the sol which, during the spinning stage, are more able to interpenetrate and then to give rise to more cross-linked structures, capable of withstanding the capillary pressure developing during the film drying. Denser species, originating by simple base addition to a solution of In^{3+} ions and by subsequent peptization, may be less cross-linked and hence less resistant to the drying stress. Actually, this phenomenon is not so evident in the case of In_2O_3 as it is for other sols derived from inorganic precursors; nevertheless, the addition of acetylacetone has clear beneficial effect on the film uniformity. To understand the actual structure of the two starting solutions and of their mixtures, a systematic characterization was undertaken by FTIR spectroscopy. Figure 1 reports the FTIR curve related to a pure In_2O_3 sol, while Table 1 contains the peaks assignment. Following refs 23 and 24, the peaks at 1570, 1527, 1273, 1016, 932, and 670 cm^{-1} are assigned

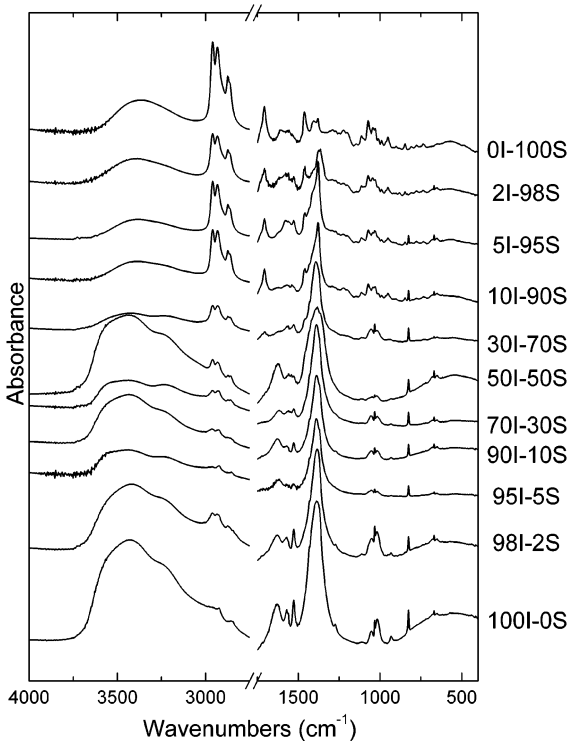

Figure 2. FTIR curves measured on sols with the indicated compositions.

to indium acetylacetonato complexes, indicating that In^{3+} ions are effectively chelated by acetylacetone. The presence of NH_3 molecules in the In^{3+} coordination sphere cannot be excluded since some bands are in characteristic positions of the metal−amine complexes.

The low-frequency flank of the curve in Figure 1, which for many inorganic oxides contains typical features due to the metal−O−metal vibrations, only displays a very broad band. It is concluded that, upon base addition, the indium ions environment is constituted by a mixture of acetylacetonato and amine ligands, to which partial hydrolysis has added OH ligands. In any case, extensive inorganic polymerization is hindered since there is no precipitation. On the other hand, as seen in Figure S1 of the Supporting Information, the FTIR curve measured on the Sn solution does not present obvious differences with respect to that of the pure precursor, excluding the O−H stretching of butanol. Thus, the mixed solutions are formed starting from weakly polymerized In_2O_3 sols and Sn(II) 2-ethylhexanoate molecules dispersed in butanol.

The result of the mixing was further studied by FTIR spectroscopy and the results are shown in Figure 2, where the compositions are indicated according to the convention introduced in the Experimental Section. It is clear that for the various compositions the curves appear as a simple sum of the curves related to the parent solutions, with relative intensities dictated by the starting proportions of the two components in the solutions. No obvious differences can be seen, in particular, as concerns the possible formation of In−O−Sn heterobonds. This result can be interpreted as a direct consequence of the chemistry of the Sn solution, where the precursor is simply dispersed in butanol without any solvolysis. Thus, during the spin coating, the solvent evaporation may drive the two components, i.e., the In_2O_3 precursor

(22) Savaniu, C.; Arnautu, A.; Cobianu, C.; Craciun, G.; Flueraru, C.; Zaharescu, M.; Parlog, C.; Pasztic, F.; Van den Berg, A. *Thin Solid Films* **1999**, *349*, 29.
(23) Thornton, D. A. *Coord. Chem. Rev.* **1990**, *104*, 173.
(24) Nakamoto, K. *Infrared and Raman Spectra of Inorganic and Coordination Compounds. Part B: Applications in Cooordination, Organometallic, and Bioinorganic Chemistry*, 5th ed.; Wiley: New York, 1997.

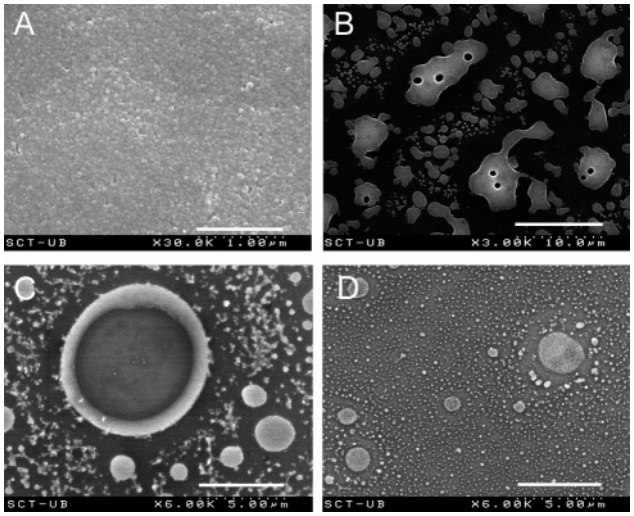

Figure 3. FE-SEM images of films heat-treated at 500 °C and with compositions 100I−0S (A), 70I−30S (B), 50I−50S (C), and 30I−70S (D). The scale-bar values are reported on the bottom of each image.

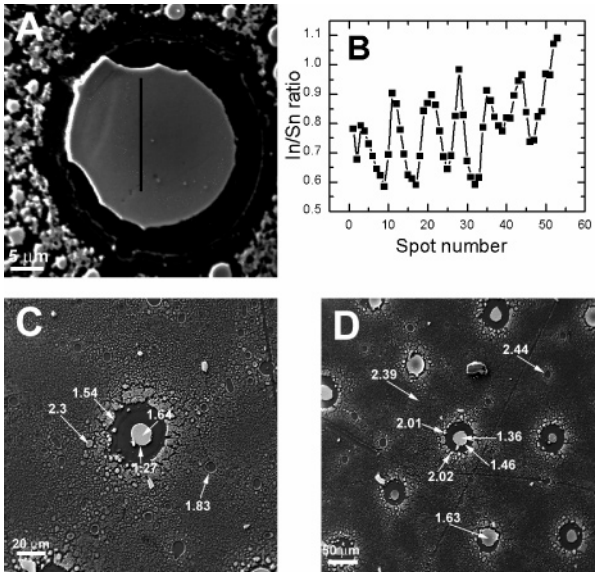

Figure 4. (A) SEM image of one of the bigger islands observed in the 50I−50S film and (B) the In/Sn atomic ratio found by Auger analysis in spots placed along the direction shown on the island; (C) lower magnification SEM image of the same film, reporting the In/Sn atomic ratio obtained from the Auger analysis in the indicated points; (D) same as (C), on a larger area.

species and the Sn(II) 2-ethylhexanoate molecules, toward eventual mutual solubility limits.

B. Study of the Film Formation and Evolution with the Heat Treatments. Due to the unusual nominal compositions of the starting sols, first of all the film morphologies were studied by FE-SEM as a function of the composition, for evidencing eventual phase separations. Figure 3 shows the FE-SEM images of selected thin films heat-treated at 500 °C. Different scales are used in order to enhance some morphological features. While the pure films show a compact and uniform morphology, constituted by close packed grains (this feature is hardly discernible for pure SnO_2 because of its small grain size, so the corresponding image is not shown), as shown for In_2O_3 in (A), films with intermediate compositions display a discontinuous morphology where large islands are dispersed in a more uniform background constituted by smaller structures. Increasing the SnO_2 concentration in In_2O_3-based films results in an enhancement of this phenomenon, as seen in (B) and (C), with the formation of larger islands that appear as droplets dispersed on the substrate. In the case of the 30I−70S film, a similar morphology is observed but the droplets are much smaller than for systems in which the In_2O_3 component is prevalent and have a rough morphology. Since the droplets and the islands appear as the most characteristic feature of the films, the elemental mapping of such structures by Auger analysis was carried out.

The analysis was limited to the 50I−50S composition as an extreme case. First of all, the mapping of a single island was carried out, as shown in Figure 4A, where we highlight the line along which the different Auger analyses (each one of them corresponding to a spot of less than 500 nm along this line) have been acquired.

The results of the Auger analysis are reported in Figure 4B, and it clearly appears that the In concentration is strongly depleted in the island, taking into account that the nominal In/Sn atomic ratio is 2 in this sample. For excluding that this result could be due to a systematic substoichiometry of the film, the analysis was carried out in various points on a larger scale, with the results shown in Figures 4C and 4D. It is evident that the In depletion is characteristic of the large islands, while the In/Sn ratio is closer to the nominal value in other points and in some cases it is beyond such value. It is worth highlighting that in the region closest to the large islands only silicon dioxide is detected.

The amount of tin that can be incorporated has shown to depend on the preparation method, as already reported for ITO powders.[16b] This result holds even for our films, where the Auger results indicate that the intrinsic properties of the starting solutions already constitute a solubility limitation. From the results described until now, in fact, the formation and the morphological evolution of the films can be outlined as follows. During the spinning stage, the solvent evaporation induces a phase separation between the two components of the starting sol, i.e., the In_2O_3 species and the molecules of the Sn precursor. A possible reason for the phase separation might be the low affinity between the polar surface of the species in the In_2O_3 sol, which, from the FTIR results, contain In−OH bonds, and the less polar molecules of the Sn(II) 2-ethylhexanoate. In the sol stage the low affinity is overcome by the presence of alcoholic solvents. In this way, the film is constituted by regions differently enriched in each of the two components. In the film with 50I−50S composition, in which this situation is enhanced, the presence of regions with different chemical structure interrupts the cross-linking between the In_2O_3 species. Thus, the film is less resistant to the drying stresses originating during the spinning stage and finally results in the dewetting of the substrate, with the formation of the typical islandlike structures. The latter, from the Auger results, are now described as the regions of accumulation of the Sn(II) 2-ethylhexanoate, characterized by low In/Sn atomic ratios and implying the presence of the other regions with the reverse behavior of the In/Sn ratio.

The samples with different compositions can then be seen as the stages of a continuous evolution of the film morphol-

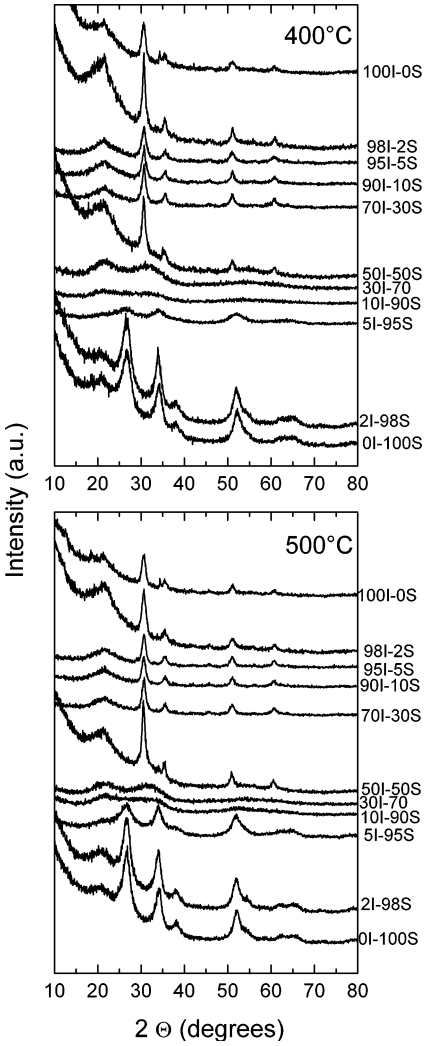

Figure 5. XRD patterns measured on thin films with the indicated compositions and heat-treated at the indicated temperatures.

ogy and adhesion, corresponding to the composition change. In particular, when SnO_2 is the prevailing phase, as in Figure 3D, an islandlike morphology is still observed, but it is characterized by smaller islands and by a more continuous appearance, with the islands that now have a granular morphology resembling that observed in Figure 3A. Since the general trends of the film formation clearly appeared, the 30I−70S composition and the others were not investigated in more detail by Auger spectroscopy, and the next step was the study of structural evolution of the films with the heat treatments.

The XRD patterns were recorded on films with various compositions and heat-treated up to 400 and 500 °C. The main features of the patterns, shown in Figure 5, are the following: (a) when crystallization is observed, it concerns only the prevailing component and in the most usual crystallographic phase, the cubic for In_2O_3 and tetragonal for SnO_2; (b) crystalline SnO_2 is not formed for 30I−70S and 10I−90S films, and for the 5I−95S film it is clearly crystallized only after heating at 500 °C; (c) crystalline In_2O_3 is formed for *I* values from 100 down to 50; (d) only a very slight shift of the diffraction peaks are observed when varying the film composition. These observations evidence a clear influence of the In_2O_3 component on the SnO_2 crystallization,

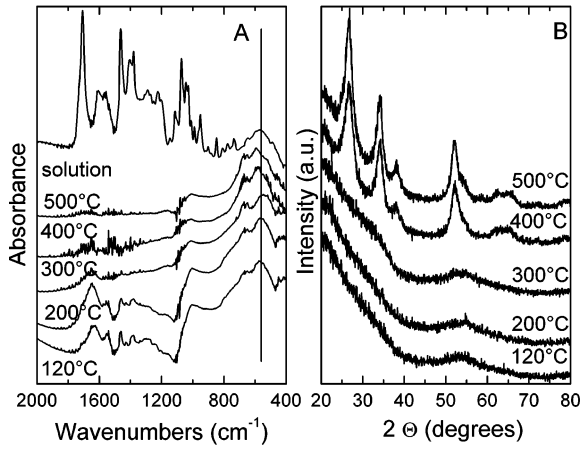

Figure 6. FTIR spectra (A) and XRD patterns (B) measured on films with 0I−100S composition as a function of the heating temperature. The vertical line in (A) is for evidencing the different peak positions in the low-frequency range as a function of the heating temperature.

but the reversal influence of SnO_2 on In_2O_3 is not observed. For explaining the asymmetric crystallization behavior of the films with respect to the composition, we referred to the different chemical structures of the In and Sn species. In fact, the In-enriched regions contain at least weakly polymerized species, eventually incorporating some Sn-containing molecules. In these regions, the In_2O_3 crystallization may occur by displacive phenomena in the partially pre-organized colloidal structures. With increasing the *I* values, the In-rich regions are larger and larger and will contain a continuously decreasing amount of Sn precursor, which will favor the In_2O_3 crystallization.

On the other hand, the Sn-rich regions are constituted by weakly bound Sn(II) 2-ethylhexanoate molecules, eventually incorporating In species or mixed with In-enriched regions. Differently from the In-rich regions, the Sn species originated from the decomposition of a molecular precursor, so they need diffusing to the nucleation centers for forming the crystallites. The diffusion of species and the formation of nucleation centers may be strongly hindered by the presence of "foreign" structures. FTIR and XRD studies on pure SnO_2 films as a function of the temperature gave further support to this hypothesis, and the results are reported in Figure 6. It is clearly seen in (A) that up to 300 °C in the low-frequency range the FTIR curves on the films resemble that of the starting solution, while the XRD patterns do not show any crystallization. After heating at 400 °C, the films are suddenly crystallized and the FTIR curves in the low-frequency region have the typical SnO_2 structure. On the other hand, as shown in ref 18, In_2O_3 thin films crystallize at lower temperatures. These results support the idea of a steplike formation of the SnO_2 structure, where first the precursor must be decomposed, providing the species that will form the final structure. Such a formation mechanism can indeed be strongly influenced by the presence of other species, by at least two possible pathways: incorporation of In ions in the SnO_2 lattice and hindering of the diffusion of the Sn species by the In-enriched islands.

With this premise, the results in Figure 5 could be interpreted as follows. Starting from the 0I−100S composition, for I values up to 2 there are no relevant effects on the

SnO_2 crystallization. When I is 5, the film must be heated to 500 °C for crystallizaiton. Since in this case the diffusion hindering effect previously described is not likely to be important, we attribute this result to the increased incorporation of In ions in the SnO_2 lattice with respect to I = 2. For I = 10 or 30, no crystallization is observed even after heating at 500 °C. In these cases, besides the incorporation of In ions in the SnO_2, which may encounter solubility limits, the presence of islands in the film structure may become more and more important. For I ≥ 50, only the In_2O_3 crystallization is always observed, apart from a small SnO_2 peak in the 50I−50S film: the In-rich regions are large enough for their crystallization to be observed, and they are not influenced by the Sn precursor which is confined in separate regions. In other works, *in general* only the presence of only crystalline In_2O_3 is reported in ITO thin films,[10b,c,11,13,15b,20,21] or only of SnO_2 when it is the prevailing component.[21] In coprecipitated powders, SnO_2 peaks have been observed for high Sn concentrations[16a] (In/Sn atomic ratio 50:50). Nevertheless, the powders formation phenomena make powders not comparable to thin films: for instance, in coprecipitation with high Sn concentrations the presence of isolated hydroxide regions becomes more and more likely. It is interesting to observe the coexistence of both In_2O_3 and SnO_2 crystallites in thin films with high Sn content (20% atomic concentration) after prolonged heat treatment at 950 °C for 2 weeks.[25] These extreme conditions were attributed to the formation of metastable ITO films, where the preparation conditions prevent the formation of segregated SnO_2 phases.[26] In our case we have just the opposite behavior, with separated regions containing the SnO_2 precursor, so it could be expected to have the formation of SnO_2 crystallites by milder treatments.

For testing this hypothesis, and the proposed explanation of the film structural transformations, it seemed then fundamental to heat-treat the thin films with I from 5 to 50 at least up to 800 °C. The aim was to check the effect of providing more energy for eventual structural transformations. The XRD patterns obtained for the films prepared in this way are shown in Figure 7.

The results show that indeed the films that were amorphous after the heat treatment at 500 °C, like those with I = 10 or 30, can be crystallized at higher temperatures. In principle, this result could indicate an influence of the In ions that are incorporated to a higher extent in the SnO_2 lattice, due to the increasing In concentration in the starting sol. Nevertheless, the peculiar pattern of the film with I = 30, where the In_2O_3 not only crystallizes but also overwhelms the crystallization of SnO_2, finally shows the fundamental role of In_2O_3-based regions in the films. Thus, we conclude that for each composition two mechanisms (incorporation of ions and diffusion hindering) may actually cooperate in determining the film structure, and that they depend on the precursor chemistry and on the film initial morphology as dictated by the chemical composition of the starting sol. While a thorough study of the incorporation of Sn or In ions in the other lattice would need at least a careful study of the electrical properties of the films, which should also be coupled with a detailed structural model of the various regions present in each film, the results of the previous studies were satisfactory in establishing at least some general principles governing the film formation in such complex systems.

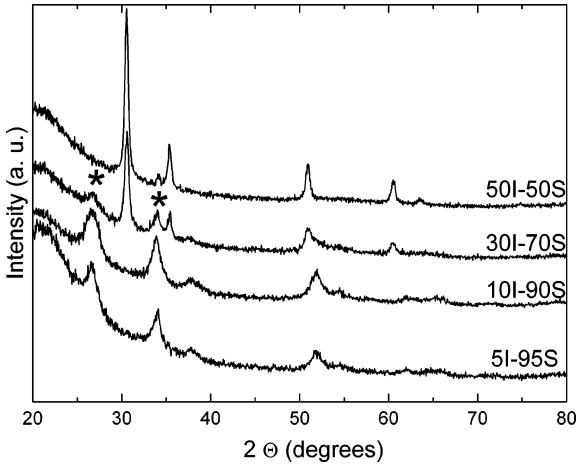

Figure 7. XRD patterns measured on thin films with the indicated compositions and heat-treated up to 800 °C. The asterisks show the residual SnO_2 peaks in films where the In_2O_3 crystallization is prevailing.

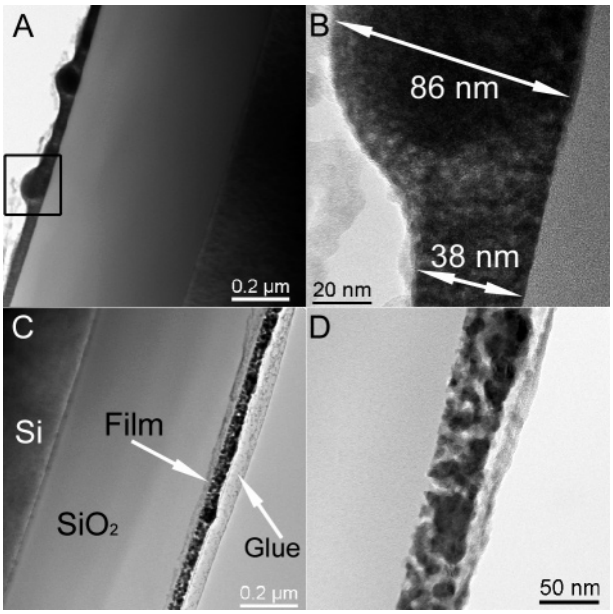

Figure 8. Low-resolution TEM images of films with 30I−70S composition, heated at 500 °C (A and B) and 800 °C (C and D). The (B) and (D) images are higher magnification images showing the following: in (B) the amorphous structure of the island highlighted in (A) and, in (D), a detail of the granular structure of the film showed in (C).

The next step was a careful structural study of the film with 30I−70S composition, due to the peculiarity of the XRD pattern showing the coexistence of two different phases. In Figure 8 the comparison is shown between a film heated at 500 °C and one heated at 800 °C. Some important differences can be readily evidenced. First of all, in Figure 8A the islands characterizing the film formation are clearly seen as spherical structures. The whole film is amorphous, as seen from HRTEM images and power spectra (FFT) obtained on

(25) Frank, G.; Köstlin, H.; Rabeanu, A. *Phys. Status Solidi A* **1979**, *52*, 231.
(26) Parent, P.; Dexpert, H.; Tourillon, G.; Grimal, J.-M. *J. Electrochem. Soc.* **1992**, *139*, 282.

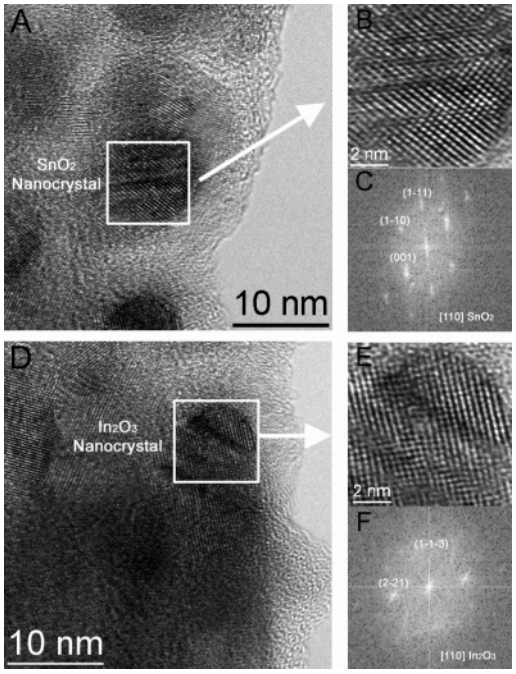

Figure 9. HRTEM images of different regions in a film with 30I−70S composition, heated at 800 °C (A and D), showing the coexistence of SnO_2 nanocrystals (B and, in C, the related power spectra (FFT)), and of In_2O_3 nanocrystals (E and, in F, the related power spectra (FFT)).

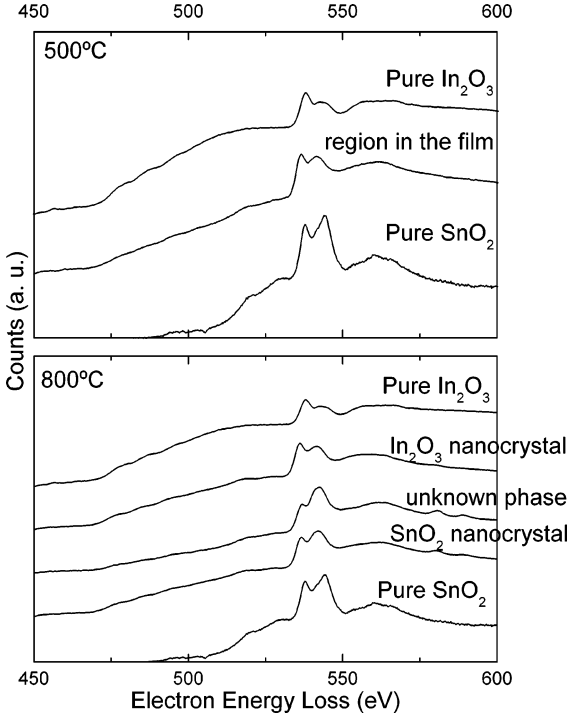

Figure 10. EELS spectra of the thin films with 30I−70S composition and heat-treated up to the indicated temperatures.

different regions in the films (Figure S2, Supporting Information). When the film is heated at 800 °C, its morphology is completely planarized, as seen from the uniform thickness in Figure 8C and the lack of the spherical structures. Actually, the FE-SEM images (see Figure S3, Supporting Information) showing larger regions of the sample evidence residual structures of the previous morphology.

Figure 8D shows that after heating at 800 °C the film is characterized by a granular structure, which was studied in detail by HRTEM. The results, shown in Figure 9, are striking since the coexistence of In_2O_3 and SnO_2 peaks in the XRD pattern of Figure 6 is clearly confirmed to be due to the simultaneous presence of nanocrystals of the two phases in the same film. Actually, the film seems to be composed of an assembly of nanocrystals with different compositions, as clearly evidenced by the EELS spectra showed in Figure 10. While in the film heated at 500 °C only one signal is seen, indicating an intermediate composition between pure SnO_2 and pure In_2O_3, in the film heated to 800 °C the EELS signal abruptly changes depending on the selected nanocrystal, indicating phases more similar to pure SnO_2 or to pure In_2O_3 but not attributable to the pure oxides or known mixtures of them.

Conclusions

In this work we have evidenced how the use of precursors characterized by a different chemistry influences all the stages of thin film formation in complex systems, starting from the eventual formation of heterobonds in the starting solution. Among the peculiar results due to the precursor chemistry, we have reported the observation of different phase grains in thin films, which is not common for several reasons: first of all, the achievement of immiscibility regions in the phase diagram is not simple with traditional physical deposition processes; second of all, even with use of chemical processes that allow the preparation of solutions with unusual compositions, the formation of separate phases may require extreme conditions, such as very high heating temperatures, which may result in the appearance of macroscopic defects in the film, such as cracking or peeling away from the substrate. We believe that in the present work the observation of the structure of Figure 9 is due to the simultaneous presence in the starting solution of two precursor species that are initially compatible, due to the solvent which is an alcohol in both cases, and that become separate during the film formation for the reasons previously explained. We remark that this work could also be seen as directed at establishing general limitations in mixing different precursors, as far as one is concerned with the obtainment of uniform and homogeneous thin films.

Acknowledgment. Mauro Epifani acknowledges the financial support from the National Council of Research (CNR) for a short-term mobility at the University of Barcelona (Spain). The Auger, SEM, XRD, and FTIR units of the Serveis Científico-Tècnics of the University of Barcelona are gratefully acknowledged for their cooperation. This work was supported by the European Union in the frame of the NANOS4 (Grant NMP4-CT-2003-001528) project.

Supporting Information Available: FTIR curves of the Sn precursor and the related solution, TEM images of the 30I−70S film heat-treated at 500 °C, and FE-SEM images of films heat-treated up to 800 °C (PDF). This material is available free of charge via the Internet at http:// pubs.acs.org.

CM0522477